

FINAL TECHNICAL REPORT
September 1, 2003, through August 31, 2005

Project Title: **A NOVEL MEMBRANE REACTOR FOR DIRECT
HYDROGEN PRODUCTION FROM COAL**

ICCI Project Number: DEV03-1
Principal Investigator: Francis Lau, Gas Technology Institute
Other Investigators: Shain J. Doong, Gas Technology Institute
 Estela Ong, Gas Technology Institute
 Mike Roberts, Gas Technology Institute
Project Manager: Ronald H. Carty, ICCI

ABSTRACT

Gas Technology Institute has developed a novel concept of a membrane reactor closely coupled with a coal gasifier for direct extraction of hydrogen from coal-derived syngas. The objective of this project is to determine the technical and economic feasibility of this concept by screening, testing and identifying potential candidate membranes under the coal gasification conditions. The best performing membranes were selected for preliminary reactor design and cost estimate. The overall economics of hydrogen production from this new process was assessed and compared with conventional hydrogen production technologies from coal.

Several proton-conducting perovskite membranes based on the formulations of BCN ($\text{BaCe}_{0.8}\text{Nd}_{0.2}\text{O}_{3-x}$), BCY ($\text{BaCe}_{0.8}\text{Y}_{0.2}\text{O}_{3-x}$), SCE (Eu-doped SrCeO_3) and SCTm ($\text{SrCe}_{0.95}\text{Tm}_{0.05}\text{O}_3$) were successfully tested in a new permeation unit at temperatures between 800 and 1040°C and pressures from 1 to 12 bars. The experimental data confirm that the hydrogen flux increases with increasing hydrogen partial pressure at the feed side. The highest hydrogen flux measured was 1.0 cc/min/cm² (STP) for the SCTm membrane at 3 bars and 1040°C. The chemical stability of the perovskite membranes with respect to CO₂ and H₂S can be improved by doping with Zr, as demonstrated from the TGA (Thermal Gravimetric Analysis) tests in this project.

A conceptual design, using the measured hydrogen flux data and a modeling approach, for a 1000 tons-per-day (TPD) coal gasifier shows that a membrane module can be configured within a fluidized bed gasifier without a substantial increase of the gasifier dimensions. Flowsheet simulations show that the coal to hydrogen process employing the proposed membrane reactor concept can increase the hydrogen production efficiency by more than 50% compared to the conventional process. Preliminary economic analysis also shows a 30% cost reduction for the proposed membrane reactor process.

Future work should be focused on improving the permeability for the proton-conducting membranes, testing the membranes with real syngas from a gasifier and scaling up the membrane size.

EXECUTIVE SUMMARY

The overall objective of this project is to develop a novel membrane reactor process for high efficiency, clean and low cost production of hydrogen from coal. The concept incorporates a hydrogen-selective membrane closely coupled with a gasification reactor for direct extraction of hydrogen from coal-derived syngas. As more than 50~60% of the final hydrogen product is generated in the gasification stage, there is great potential of maximizing hydrogen production by separating hydrogen directly from the gasifier. By configuring a hydrogen-selective membrane with a gasification reactor in a closely coupled way, both gasification reactions and hydrogen separation can be accomplished simultaneously. This concept has the potential of significantly increasing the thermal efficiency of producing hydrogen, simplifying the processing steps and reducing the cost of hydrogen production from coal. In addition, this concept can also reduce the cost of CO₂ capture for the hydrogen from coal gasification processes.

Under the sponsorships of DOE/NETL, Illinois Clean Coal Institute, and American Electric Power, a GTI-led team has been conducting the research to determine the technical and economic feasibility of this novel concept. The project team has screened, tested and identified several potential candidate membranes at the temperature and pressure conditions of coal gasification. The best performing membranes were selected for preliminary reactor design and cost estimate. The overall economics of hydrogen production from this new process was assessed and compared with conventional hydrogen production technologies from coal. The project included the following four tasks:

Task 1 – Membrane Materials Screening and Testing

The objective of this task is to determine the hydrogen separation performance for selected membranes under the temperature and pressure conditions of coal gasification.

Due to high temperature operation in the gasifier, only inorganic materials can be considered for this application. Dense ceramic membranes of perovskite type, which possess a unique property of conducting both protons and electrons, represent one group of promising inorganic membranes for use in high temperature membrane reactors. Under a pressure gradient of hydrogen across the membrane, only hydrogen can permeate through it, resulting in a pure and clean hydrogen product.

To evaluate the performances of the candidate membranes at the gasification conditions, a high temperature/high pressure hydrogen permeation unit was constructed. The unit was designed to operate at temperatures up to 1100°C and pressures to 60 bars for evaluation of ceramic membranes such as mixed protonic-electronic conducting membrane.

Several proton-conducting perovskite membranes based on the formulations of BCN (BaCe_{0.8}Nd_{0.2}O_{3-x}), BCY (BaCe_{0.8}Y_{0.2}O_{3-x}), Eu-doped SrCeO₃ (SCE) and SrCe_{0.95}Tm_{0.05}O₃ (SCTm) were successfully tested in a new permeation unit at

temperatures between 800 and 1040°C and pressures from 1 to 12 bars. These membranes were made by either tape casting or uniaxial pressing methods. The experimental data confirm that the hydrogen flux increases with increasing hydrogen partial pressure at the feed side. The hydrogen flux, however, declines with increasing hydrogen pressure beyond about 6 bars, presumably due to the limited equilibrium solubility of hydrogen in the membrane. The highest hydrogen flux measured was 1.0 cc/min/cm² (STP) for the SCTm membrane at 3 bars and 1040°C. The flux of the SCTm membrane appears to be adequate for the membrane module design.

The chemical stability of the perovskite membranes was also evaluated by testing the reactions of a Zr-doped perovskite with respect to CO₂ and H₂S in a TGA (Thermal Gravimetric Analysis) unit. The Zr-doped perovskite showed better resistance to CO₂ and H₂S than the BCN or SCE membrane.

Task 2 – Conceptual Design of Membrane Reactor

This task is to investigate how a membrane reactor can be configured with a coal gasifier. The conceptual design is based on the membrane testing results from Task 1 and a modeling approach.

A conceptual design of the membrane reactor configuration for a 1000 tons-per-day (TPD) coal gasifier was conducted. The design considered a tubular membrane module located within the freeboard area of a fluidized bed gasifier. The membrane ambipolar conductivity was based on the value calculated from the measured permeation data. A membrane thickness of 25 micron was assumed in the calculation. GTI's gasification model combined with a membrane reactor model was used to determine the dimensions of the membrane module. It appears that a membrane module can be configured within a fluidized bed gasifier without substantial increase of the gasifier dimensions.

Task 3 – Process Evaluation and Flow Sheet Development

The objective of this task is to compare the performances for several hydrogen from coal gasification processes with and without the membrane reactors.

The commercial flowsheet simulator HYSYS was used to calculate material and energy balances based on four hydrogen production processes from coal using high temperature membrane reactor (1000°C), low temperature membrane reactor (250°C), or conventional technologies. The results show that the coal to hydrogen process employing both the high temperature and the low temperature membrane reactors can increase the hydrogen production efficiency (cold gas efficiency) by more than 50% compared to the conventional process. Using either high temperature or low temperature membrane reactor processes also result in an increase of the cold gas efficiencies as well as the thermal efficiencies of the overall process.

Task 4 – Economic Evaluation for Overall H₂ Production Process

Based on the flowsheet results, a preliminary economic analysis was conducted to estimate the hydrogen product cost for various process schemes with and without the membrane reactor. Capital costs for process equipment were adopted from those reported in the literature. The membrane cost was assumed to meet the DOE's cost target of \$100/ft². The results show that the coal to hydrogen process employing both the high temperature and the low temperature membrane reactors can reduce the hydrogen cost by about 30% compared to the conventional process.

At a scoping level, the project demonstrated the technical feasibility and the economic benefit of the proposed membrane reactor concept for hydrogen production from coal gasification. However, significant technical challenges still need to be overcome in order for the technology to be successful. The following are recommendations for future work:

- Improve the hydrogen permeability by minimizing the membrane thickness and increasing the material conductivity.
- Improve the chemical and mechanical stability of the membrane materials.
- Conduct permeation testing with simulated syngas
- Conduct permeation testing with real syngas from a coal gasifier
- Scale up the size of the membrane disks. Samples as large as 1.25" diameter disks have been routinely prepared in this program. Much bigger sizes will be needed for future commercial applications.

OBJECTIVES

The overall objective of this project is to develop a novel membrane reactor process for high efficiency, clean and low cost production of hydrogen from coal. The concept incorporates a hydrogen-selective membrane closely coupled with a gasification reactor for direct extraction of hydrogen from coal-derived syngas. The specific objective of the project is to determine the technical and economic feasibility of using the membrane reactor to produce hydrogen from coal. Potential membranes are evaluated under high temperature and high pressure conditions of coal gasification and selected for preliminary reactor design. The overall economics of hydrogen production from this new process is assessed and compared with other hydrogen production technologies from coal.

The project includes the following four tasks:

Task 1 – Membrane Materials Screening and Testing

The objective of this task is to determine the hydrogen separation performance for selected membranes under the temperature and pressure conditions of coal gasification. This task involves design and construction of a high pressure permeation unit and testing of the candidate membranes.

Task 2 – Conceptual Design of Membrane Reactor Membrane Reactor

This task is to investigate how a membrane reactor can be configured with a coal gasifier. The conceptual design is based on the membrane testing results from Task 1 and a modeling approach.

Task 3 – Process Evaluation and Flow Sheet Development

The objective of this task is to compare the performances for several hydrogen from coal gasification processes with and without the membrane reactors. The advantages of using the membrane reactors in the hydrogen from coal gasification processes are demonstrated in terms of the hydrogen cold gas efficiency and the thermal efficiency.

Task 4 – Economic Evaluation for Overall H₂ Production Process

The hydrogen costs from various process schemes incorporating the membrane reactor concept are compared with the current technologies from coal gasification without the use of the membranes. This task would demonstrate the ultimate benefit of the proposed membrane reactor concept.

INTRODUCTION AND BACKGROUND

One of the active research areas in reducing the hydrogen cost from coal gasification processes is the development of high temperature membranes that can be designed to

separate hydrogen from the coal-derived syngas. This type of membrane system is primarily targeted as a membrane reactor at 250-500°C for the water-gas-shift reaction to convert the syngas to hydrogen. While pure hydrogen is generated directly from the membrane shift reactor, the remaining gas containing mostly CO₂ and some CO and H₂ is sent to a gas turbine to combust with oxygen for power generation. Recent studies performed by Parsons [1] and Mitretek [2] showed that the hydrogen plant employing this type of membrane system could achieve a significant reduction of hydrogen cost, compared with the conventional hydrogen plant for coal gasification.

GTI has developed a novel concept of a membrane reactor by incorporating a hydrogen-selective membrane near or within a gasifier for direct extraction of hydrogen from the coal-derived syngas. As more than 50~60% of the final hydrogen product is generated in the gasification stage, there is great potential of maximizing hydrogen production by separating hydrogen directly from the gasifier. This concept has the potential of significantly increasing the efficiency of producing hydrogen and simplifying the processing steps by reducing/eliminating the downstream shift reactor, separation and purification operations for the conventional gasification technologies. Figure 1 shows a simplified process diagram for the novel membrane gasification reactor, in comparison with the conventional gasification process for hydrogen production from coal.

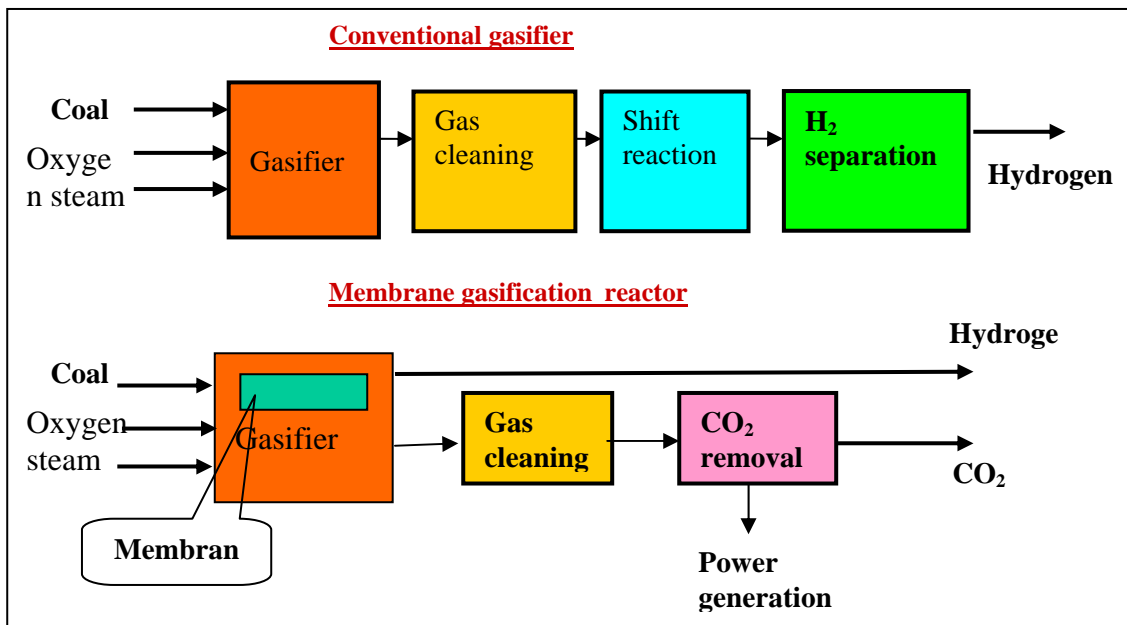


Figure 1. Hydrogen production from coal gasification based on the conventional gasifier and the novel membrane gasification reactor concept

Due to high temperature operation in the gasifier, only inorganic materials can be considered for this application. Dense ceramic membranes of perovskite type, which possess a unique property of conducting both proton and electron, represent one group of promising inorganic membranes for the use in the high temperature membrane reactors. Under a pressure gradient of hydrogen across the membrane, only hydrogen can permeate through it, resulting in a pure and clean hydrogen product. The perovskite membranes

may not be suitable for low temperature (<500°C) membrane shift reactor applications. The best working temperature range, 700~1200°C of this type of material is ideal for the membrane gasification reactor applications proposed in this project.

To confirm the feasibility of this novel concept, the project team has screened and tested several potential candidate membranes under high temperature and high pressure coal gasification conditions. In addition to experimental testing, a modeling approach was also used to examine the expected performances of the membrane gasification reactor for hydrogen production from coal. The feasibility of configuring a membrane module within a gasifier was investigated. Based on the performance of the membrane reactor, several hydrogen from coal gasification processes with and without the membrane reactors were developed and evaluated by flowsheet simulation. Economic analysis was also conducted for the different coal to hydrogen processes. The advantages of using the membrane reactors for the hydrogen from coal gasification processes were demonstrated in terms of the thermal efficiency of the process as well as the hydrogen product cost.

EXPERIMENTAL PROCEDURES

Hydrogen Flux Measurement in High Pressure Permeation Unit

As coal gasification for hydrogen production occurs at temperatures above 900°C and pressures above 20 bars, it is critically important to evaluate the hydrogen flux of the candidate membrane materials under these operational conditions. To this end, a high pressure/high temperature permeation unit has been constructed. The unit is capable of operating at temperatures and pressures up to 1100°C and 60 bar respectively. The unit can allow screening and testing of the membrane materials at more realistic gasification temperature and pressure conditions. The permeation assembly consists of a permeation cell, a surrounding cylindrical heater, and an enclosing pressure vessel. A simplified schematic illustrating the concept of the permeation cell design is shown in Figure 2. The membrane to be tested, which is in a disc form of about 2 cm in diameter, is attached or cemented to a holding tube. A hydrogen gas flows through the upper inner tube and after in contact with the membrane, exits the system as a non-permeate gas diverted by an outer tube. An inert sweeping gas passing through the lower inner tube is used to sweep the hydrogen permeate from the membrane. Therefore, the pressures on both sides of the membrane can be adjusted to be equal, which would make the membrane sealing less difficult. A glass-based sealant material is used to seal the membrane along the edge of the metallic holding tube.

The hydrogen content of the permeate is analyzed by a GC to determine the hydrogen flux through the membrane. The inner tube, outer tube and the membrane holding tube are made of Inconel material for its good resistance to heat and easy machining and welding. The entire permeation cell assembly is heated by a cylindrical heater, which is enclosed in a pressure vessel purged with inert gas. Figure 3 is a photo of the new permeation unit.

Before testing the membranes in the high pressure unit, helium was introduced to the feed side of the membrane while nitrogen was used in the permeate side as a sweeping gas to check the leakage across the membrane or the sealing material. Absence of helium in the permeate stream indicated good quality of the membrane and the seal. Pure hydrogen or hydrogen/helium mixture was used in the feed with flow rates generally in the order of 1000 cc/min. The flow rates of sweeping nitrogen varied from 80 cc/min to about 380 cc/min to generate about 1% hydrogen compositions in the permeate stream. The data were obtained at pressures up to about 12 bar and temperatures to 950°C.

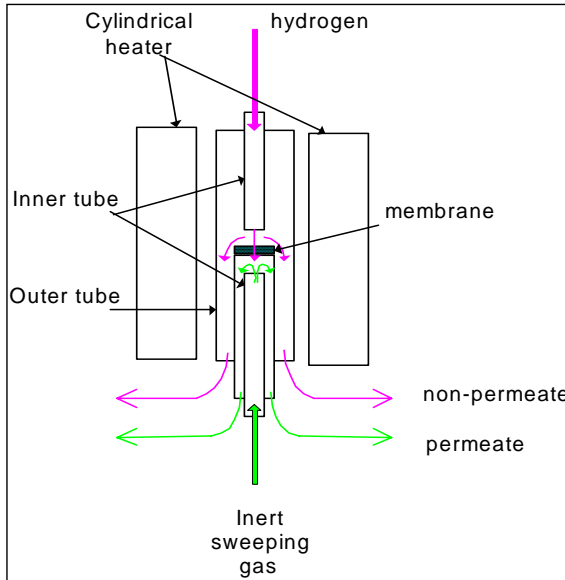


Figure 2. A schematic showing the permeation cell of the high temperature/high pressure membrane permeation unit



Figure 3. Photo of high temperature/high pressure membrane permeation unit

Membrane Material Fabrication

BCN Membrane

Nd-doped BaCeO_3 was selected as the candidate membrane for testing because BCN ($\text{BaCe}_{0.9}\text{Nd}_{0.1}\text{O}_{3-x}$) was shown in the literature to be among the highest proton conductive materials of the perovskite [3]. Two BCN membranes, one unsupported and the other supported, were fabricated. The unsupported membranes (0.2 mm in thickness) was prepared by the tape casting method, followed by sintering at 1450 to 1550°C for 2~3 hours. The supported membrane was prepared by a combination of the tape casting and the uniaxial pressing techniques. A thin (0.25 mm) membrane was first made by the tape casting process. Another thick (0.25 to 0.5 mm) membrane tape with 20 volume percent of an organic pore former was then prepared as a membrane support. The two membrane tapes were pressed together to form a laminate. The laminate was then heated to 1450-1550°C to sinter and densify the thin membrane layer and create a porous support layer of

about 0.33 mm with 31% porosity. The dense layer of the supported membrane sample was 0.2 mm. Additional details about membrane fabrication can be available in a previous ICCI project report [4].

SCE Membrane

The SCE membranes were fabricated by the tape casting method using the powders supplied from the laboratory of Professor E. Wachsman of University of Florida. Two SCE membranes, one with 10% Eu doping (SCE-10) and the other with 20% Eu doping (SCE-20) were successfully made and tested in the high pressure permeation unit. The thickness of the membranes was about 0.3 - 0.4 mm.

SCTm membranes

Three membrane disks of SCTm were prepared by the research group of Professor Jerry Lin of Arizona State University (formerly with University of Cincinnati). These are pressed membrane disks with a diameter of about 2 cm and a thickness of about 1.7 mm. These disks have required perovskite structure for proton conduction based on XRD analysis. Two of the membrane samples were tested in the GTI's high pressure permeation unit.

RESULTS AND DISCUSSION

Task 1 – Membrane Materials Screening and Testing

Hydrogen Permeation Data for Perovskite Membrane

BCN membranes

The hydrogen permeation testing results are shown in Figure 4 and 5 for the unsupported and the supported BCN membranes respectively. During the experiment, the dense layer of the supported membrane was facing the feed side and the porous support layer was on the permeate side. Despite the same thickness of the dense layer, the hydrogen fluxes for the unsupported membrane are slightly higher than the supported one probably due to the additional mass transfer resistance in the porous support layer. This is the first time that the hydrogen permeation data at high pressures (> 1 bar) for the mixed protonic-electronic conducting materials have been reported. Because of the higher operating pressures, the hydrogen flux generally is about one order of magnitude higher than those reported in the literature.

The hydrogen flux increases with the increasing hydrogen partial pressure in the feed and appears to reach a maximum at about 6 bar, after which the flux starts to drop. The pressure probably affects the hydrogen flux through two mechanisms: (1) providing the driving force of the permeation by the hydrogen partial pressure difference across the membrane and (2) affecting the conductivity by the different proton and electron concentrations or proton diffusivities inside the perovskite membrane due to the different

hydrogen pressures. Further study looking into this peculiar phenomenon using a detailed membrane permeation model seems to indicate that the decreasing flux above 6 bars is due to the limitation that the hydrogen solubility within the membrane already reaches a maximum or saturation at a pressure above 6 bar [5].

Figure 5 also shows that the flux increases with the increasing hydrogen concentration in the feed side. This is simply due to the increasing hydrogen partial pressure difference across the membrane, which results in an increasing flux. The data were obtained at 7.8 bars with 20, 60 and 100% hydrogen with balance of He in the feed side.

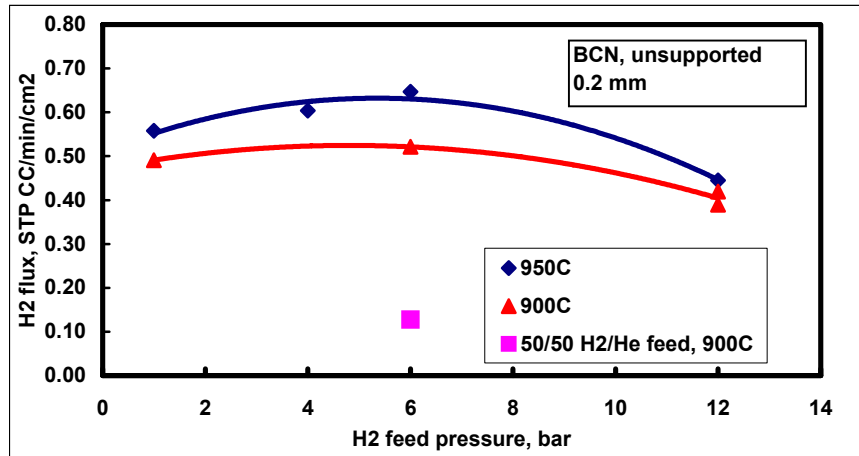


Figure 4. Hydrogen flux measured from the high pressure permeation unit for the unsupported BCN membrane

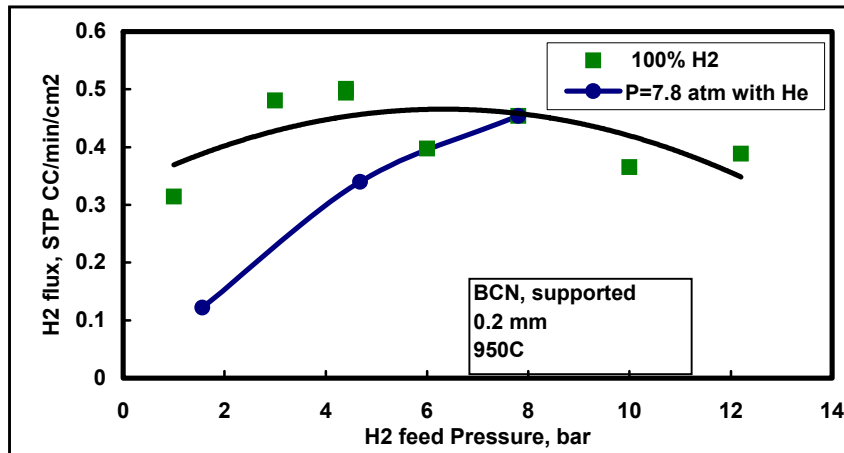


Figure 5. Hydrogen flux measured from the high pressure permeation unit for the supported BCN membrane

As expected, the hydrogen flux increases with the increasing temperature as shown in Figure 6 for the unsupported BCN membrane. The calculated activation energy is about 11.8Kcal/mole. Activation energy of 12 Kcal/mole for the proton conductivity of BCN material in the presence of steam was reported in the literature [6]. The data of the SCTm membrane in Figure 6 will be discussed later.

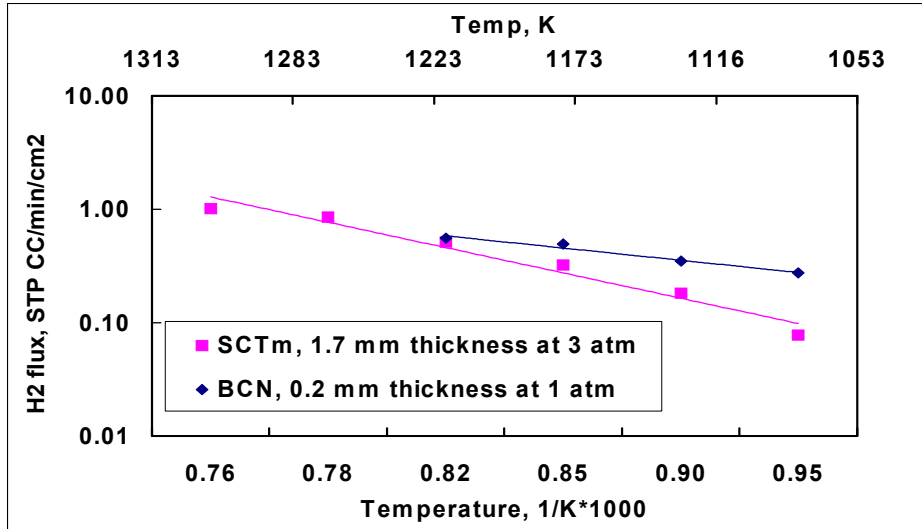


Figure 6. Hydrogen permeation data for the unsupported BCN and the SCTm at different temperatures

SCE membrane

The measured hydrogen fluxes for the SCE-10 (10% Eu doping in SrCeO₃) were shown in Figure 7 under different nitrogen sweeping flows. The hydrogen flux appears to increase with the increasing sweeping flow rate. A high sweeping flow can eliminate or reduce the mass transfer resistance in the gas phase of the permeate side. An insufficient sweeping gas flow would create a concentration gradient in the gas phase next to the permeate side of the membrane. Therefore, the measured flux increases with the flow rate of the sweeping gas and reaches a constant value eventually. The hydrogen flux for this membrane of 0.4 mm thickness is about 0.35 STP cc/min/cm² at 6 bars and 900°C with 100% hydrogen in the feed. The hydrogen flux of the SCE-10 membrane at 12 bars and 900°C with 100% hydrogen in the feed was also measured at 0.22 cc/min/cm², which is lower than the flux at 6 bars. This pressure dependence is similar to the BCN membrane.

Figure 8 is the hydrogen flux for the SCE-20 membrane at three different pressures for a hydrogen feed of 100% at 950°C. The hydrogen fluxes go through a maximum with the hydrogen feed pressure. Again, this is very similar to the data of the BCN membranes shown in Figure 4 and 5.

The hydrogen flux for the SCE-20 membrane is about 0.38 STP cc/min/cm² at 6 bars and 950°C with 100% hydrogen in the feed. No significant difference in the flux was observed between the two membranes with the different Eu dopings. The fluxes generally are lower than the BCN membranes obtained in Figure 4 and 5.

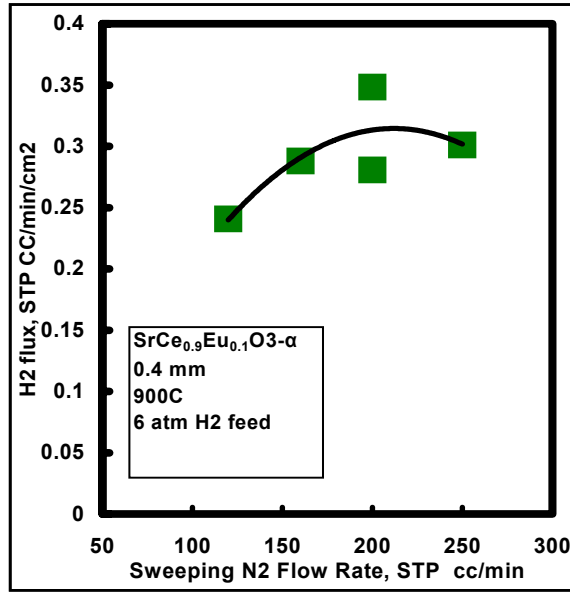


Figure 7. Hydrogen permeation flux for SCE-10 membrane measured from high-pressure permeation unit

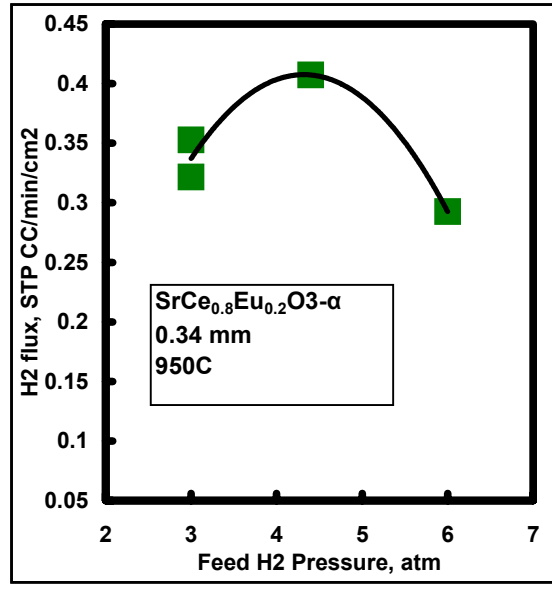


Figure 8. Hydrogen permeation flux for SCE-20 membrane measured from high-pressure permeation unit

SCTm membrane

The hydrogen permeation results for the SCTm membrane at 950°C are summarized in Figure 9 for the different hydrogen feed partial pressures. The hydrogen flux increases with the increasing feed pressure up to about 5 bar and then decreases with the pressure, as shown in Figure 9 by the curve noted with 100% H₂. With 60% hydrogen in the feed (balance of helium), the hydrogen fluxes still go through a maximum with respect to the hydrogen partial pressure in the feed, as shown by the curve with 60% H₂ (triangle points). Also shown in the figure is the effect of the hydrogen compositions in the feed on the flux at 8.14 bars. The hydrogen compositions in the feed are 20, 40, 60, 80 and 100% for this curve with the diamond points. As expected, the flux increases with the increasing composition or the partial pressure of hydrogen in the feed. Similar effect of the hydrogen compositions at 1 bar pressure is shown in the same figure. The hydrogen compositions are 100%, 60% and 20% at 1 bar for the curve with the open circles. The measured hydrogen flux with 20% hydrogen in the feed at 1 bar is also close to the literature data reported by Qi and Lin [7].

The second SCTm membrane was tested with a pure hydrogen feed at 950°C and various pressures. The hydrogen fluxes measured from this membrane are also shown in Figure 9. As can be seen, some of the data from the first membrane can be reproduced by the second membrane.

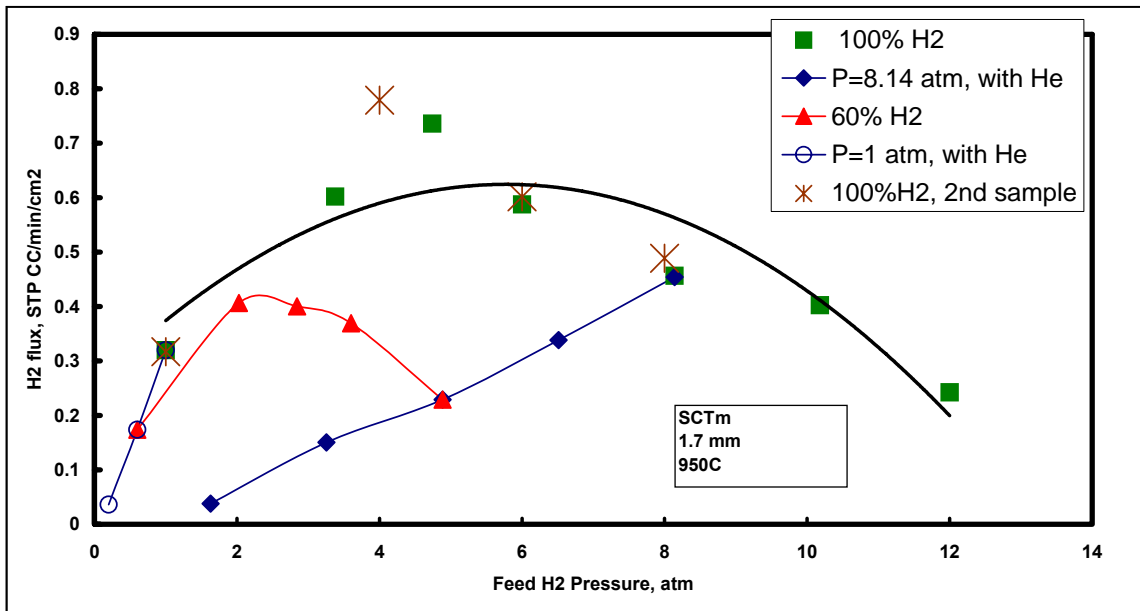


Figure 9. Hydrogen flux for the SCTm membrane at different H₂ partial pressures

If the membrane thickness is taken into consideration, the SCTm membrane (thickness 1.7 mm) shows much higher flux than the SCE membranes (thickness 0.3-0.4 mm). The fluxes are also higher than the BCN membranes reported in Figure 4 and 5. The SCTm membrane needs to be investigated further.

Additional data for the temperature dependency of the hydrogen flux for the SCTm membrane are shown in Figure 6 with 100% hydrogen in the feed at a pressure of 3 bars. The calculated activation energy for the SCTm membrane is about 27 Kcal/mole, which is higher than the BCN membrane. At higher temperatures, above 1000°C, the hydrogen flux of the SCTm membrane is higher. At temperatures below 1000°C, the BCN membrane gives higher flux.

After the reproducibility runs, the 2nd SCTm membrane was tested under continuous hydrogen feed at 1 bar for over 250 hours. The temperature was between 1010 and 1030°C and the permeate side was swept using nitrogen gas. The testing results are shown in Figure 10 for both the flux and the temperature. The hydrogen flux actually drifted upwards because the temperature was not exactly maintained at a constant value. After manually decreasing the temperature, the hydrogen flux returned back to about the same value as the beginning. A helium leak checking was also performed at the 120th hour, with an interruption of hydrogen flow of about 2 hours, to verify no deterioration of the leakage. This long term test indicates that the perovskite membrane has good thermal stability under reducing conditions in the hydrogen barsphere. The chemical stability of the perovskite membrane under the coal-derived syngas conditions, however, still needs to be tested.

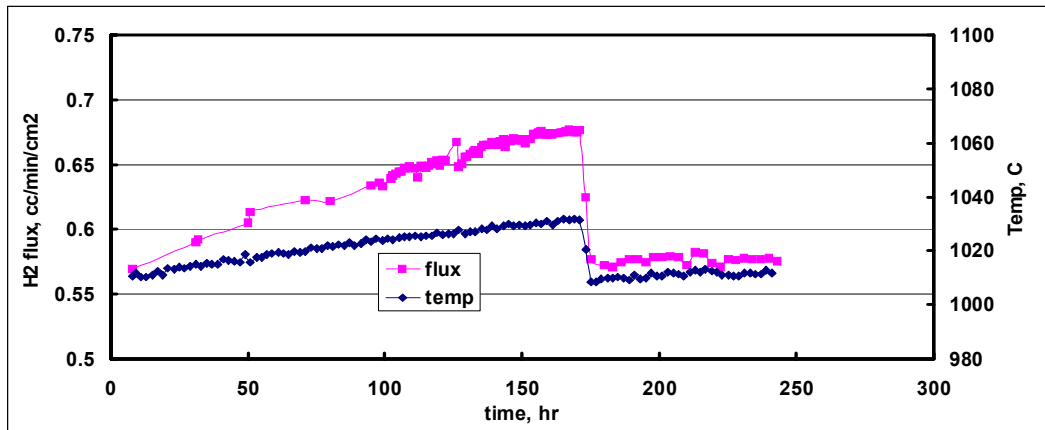


Figure 10. Hydrogen permeation testing for the SCTm membrane at 1 bar with pure hydrogen in the feed and nitrogen sweep in the permeate side

SEM and EDS Analysis of SCTm Membranes

The SCTm membrane showed the highest hydrogen flux among the membranes tested in this project. One of the tested SCTm samples was characterized by SEM (Scanning Electron Microscope) and EDS (Energy Dispersive Spectra) to investigate the structure integrity after permeation. The SEM analysis for the cross section of the tested sample after permeation shows light colored materials present between the grains towards the feed side, as shown in Figure 11(a). In comparison, a cross section near the permeate side is shown in Figure 11(b), where little light color regions can be seen.

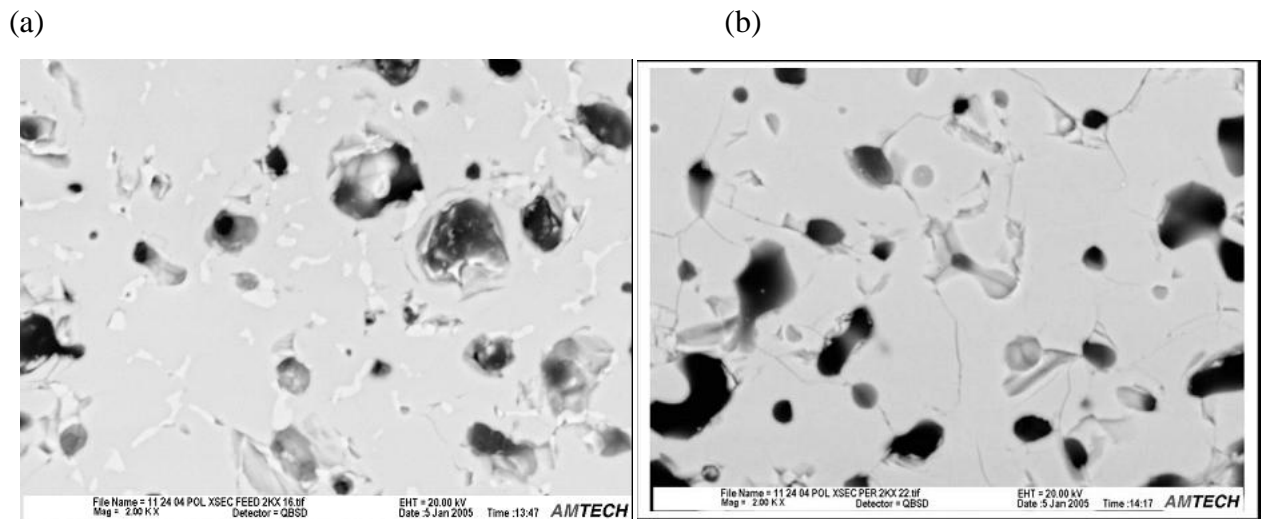


Figure 11. SEM micrographs for the membrane cross section near the feed side (a) showing light colored grain boundaries, and near the permeate side (b) showing little presence of light colored areas

To detect the elements present in the light colored areas, EDS was used with the electron beam pointed to the grain bulk and the grain boundary regions separately. The relative concentration of the elements between the grain bulk and the grain boundary areas can then be determined. The EDS spectra of the two areas are shown in Figure 12. The light colored material along the grain boundary is rich in Ce (Figure 12-a) while the bulk is richer in Sr (Figure 12-b). Presumably, cerium oxide could be separated from the perovskite structure and deposited along the grain boundaries. Because the feed side of the membrane had been encountered with pure hydrogen at pressures during the permeation testing, the perovskite could have been partially reduced by hydrogen to cause the phase separation. The phase separation was not visibly seen in the SEM graph for the permeate side of the membrane, perhaps due to the low hydrogen partial pressure in the permeate side.

A fresh sample of the SCTm membrane was examined by Professor J. Lin of Arizona State University. The SEM image of the membrane cross section for the fresh sample is shown in Figure 13. The fresh sample has much clearer grain boundary and more faceted grain surface than the permeation-tested sample, which has almost invisible grain-boundary (see Figure 11). This difference could be caused by the additional sintering effects for the permeation-tested sample, which was subjected to elevated temperatures for the permeation test for an extended period of time. Although the permeation temperature (around 900°C) may not be as high as the normal sintering temperature (>1200°C), the actual sintering effects during permeation could be more pronounced due to the presence of hydrogen (more like a reactive sintering). If the “reactive sintering” during permeation test actually occurs, the membrane can be further densified and its mechanical strength could be enhanced. This still needs to be verified.

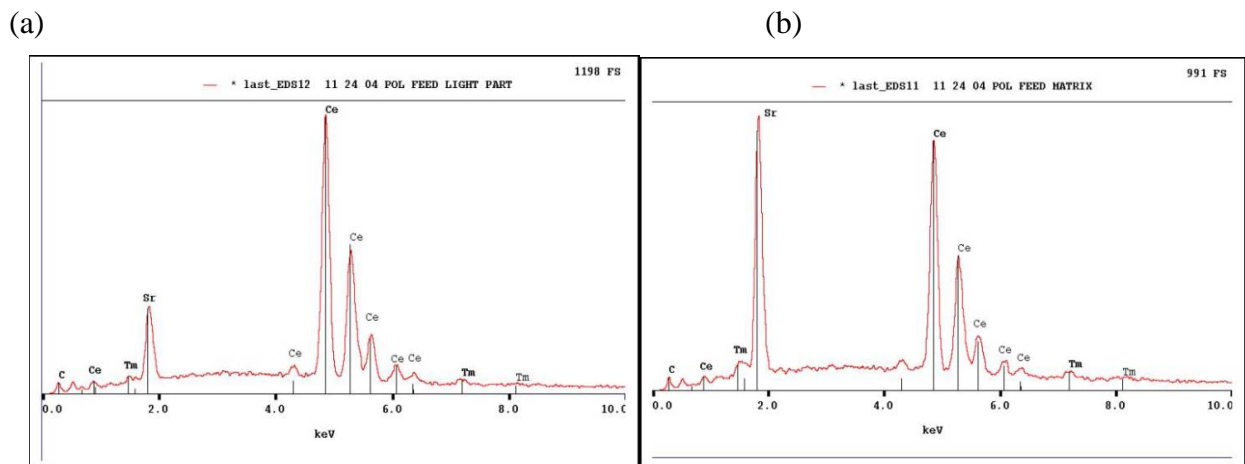


Figure 12. EDS pattern of (a) the light colored region or grain boundary, and (b) the bulk region or grain interior, from the SEM micrograph shown in Figure 11

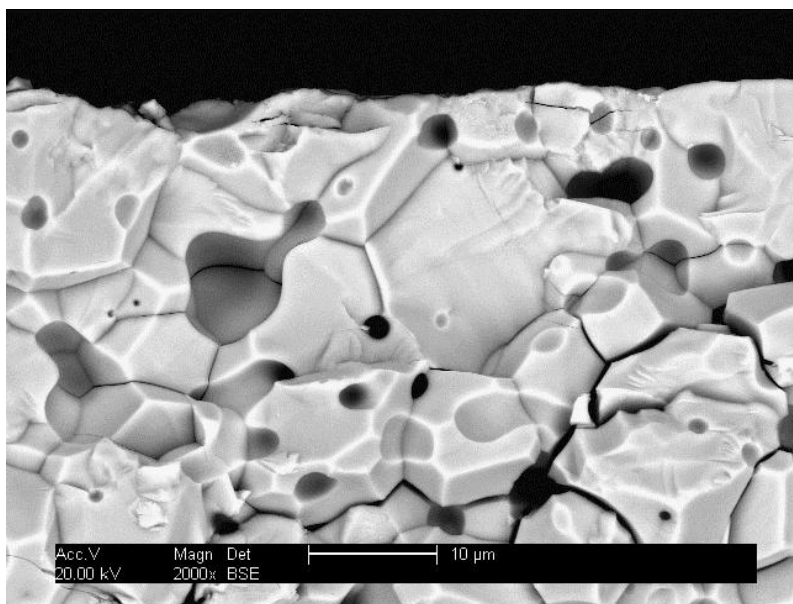


Figure 13. Microstructure of the fresh SCTm membrane at magnification of 2000X

Zr-doped Perovskite

Literature survey indicates that the Zr doped perovskite materials have improved stability for CO₂ [8,9,10]. In particular, the Yb-doped perovskite shows little reduction of the conductivity by the introduction of Zr [8]. Therefore, the Zr and Yb doped barium cerate perovskite powder; BaCe_{0.5}Zr_{0.4}Yb_{0.1}O_{3-x} (BCZY) was fabricated into dense membrane disks and tested in the Thermo Gravimetric Analyzer (TGA) unit for the chemical stability with respect to CO₂ and H₂S. The reaction of BCZY disk with CO₂ is shown in Figure 14 in comparison with the BCN and SCE membranes. The tests were conducted at 950°C and 10 bar with 10% CO₂ in He. Figure 14 shows the amounts of CO₂ that reacted with one mole of perovskite compound. The reaction of BCN with CO₂ resulted in the formation of BaCO₃, which was confirmed by the chemical analysis of the reacted membrane sample. As can be seen, the Zr doped perovskite or BCZY has better stability with CO₂ than BCN or SCE. BCZY in the form of powders was also tested in the TGA and showed better CO₂ stability than the powder form of the BCN or SCE (data not shown here). Further, the disk form of the material has better stability than the powder form.

The chemical stability of BCZY with respect H₂S is shown in Figure 15. The tests were conducted at 950°C and 10 bar with 0.1% H₂S in H₂. In comparison with the BCN powder and the BCN membrane disks, the BCZY shows improved resistance to H₂S. As expected, the BCN disk has better chemical stability than the powder. XRD analysis of the reacted sample indicated the presence of the perovskite structure with the formation of neodymium oxide sulfide, Nd₂O₂S and barium sulfide, BaS. Presumably, H₂S was adsorbed chemically on the surface of the membrane, forming the above sulfide compounds.

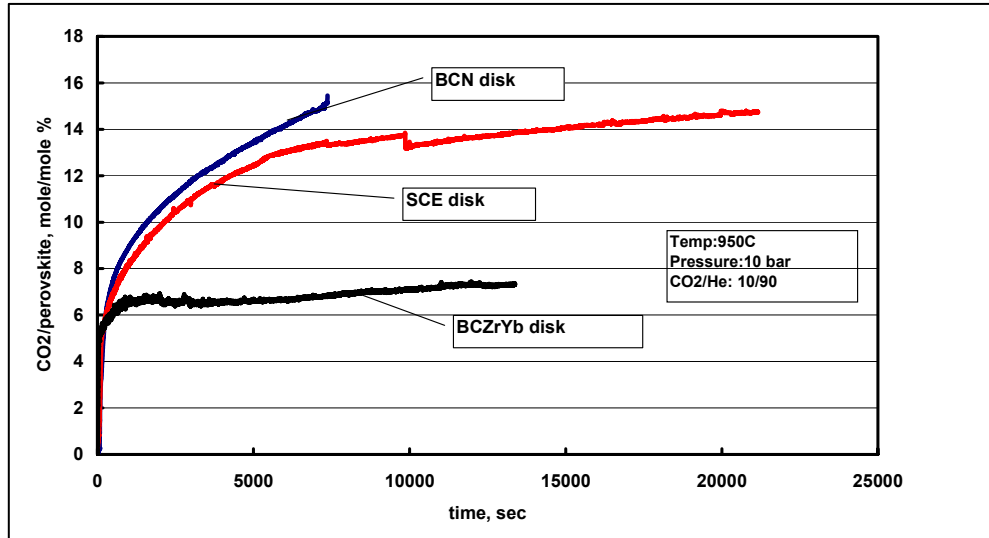


Figure 14. Thermo gravimetric results for the reaction of CO_2 with Zr-doped BCZY, BCN and SCE membrane disks

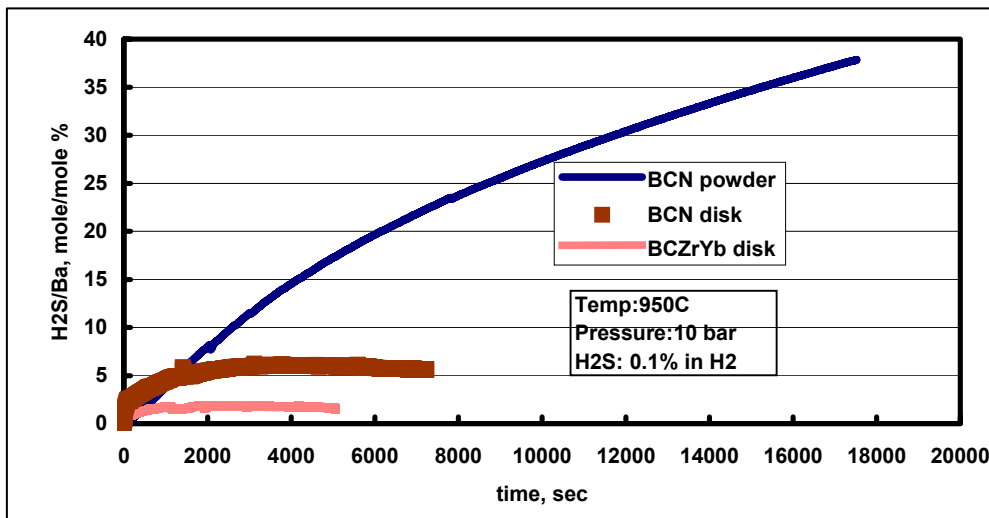


Figure 15. Dense membrane of Zr doped perovskite shows stronger resistance to H_2S than BCN membrane or powder

The Zr-doped perovskite is expected to have lower conductivity, hence lower hydrogen flux. Material development in increasing the conductivity and reducing the membrane thickness will be required to raise the flux of the Zr-doped materials.

Task 2 – Conceptual Design of Membrane Reactor

A conceptual design of the membrane reactor configuration for a 1000 TPD coal gasifier was conducted to investigate the feasibility of placing a membrane reactor within a gasifier. The design considered a tubular membrane module located within the freeboard area of a fluidized bed gasifier as shown in Figure 16. The coal syngas generated in the gasification zone at the lower section of the fluidized bed enters the membrane reactor

module. To further protect the membrane material from the solid particles, each membrane tube, as a provision, can be enclosed within a ceramic filter tube as shown in Figure 17. Thus, only gas species can enter the annular section of the tube. As the filter tubes are sealed at the bottom, the syngas will continue traveling upwards inside the annular part. Due to the selective property of the membrane material, hydrogen will permeate through the inner membrane tube and flow upwards to the top plenum chamber before exiting the gasifier. The non-permeate gas or retentate will be collected at another plenum chamber below the hydrogen chamber and exit through the side ports of the gasifier.

Alternatively, the membrane module can be located outside the gasifier, e.g. just after the cyclone of the gasifier to be closely coupled with the gasifier in terms of the syngas temperature and pressure. This arrangement would not affect the sizing of the membrane module.

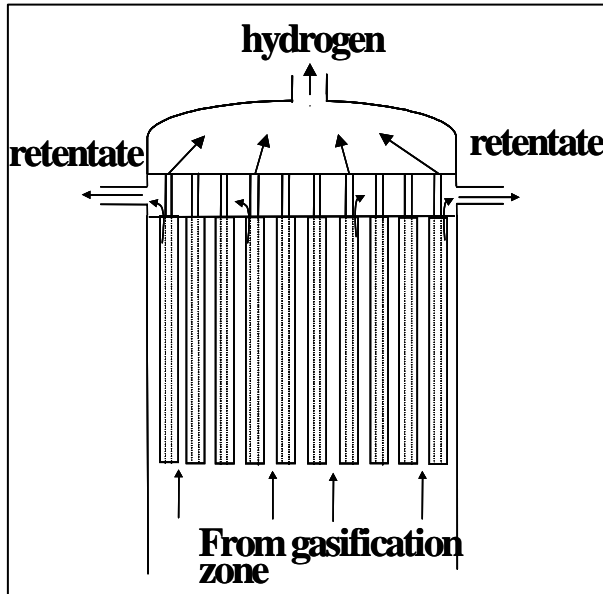


Figure 16. Schematic diagram of a tubular membrane module within a fluidized bed gasifier

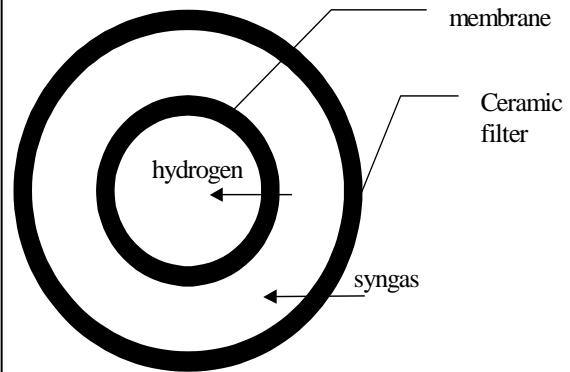


Figure 17. Enlarged cross section of a membrane tube

To estimate the required membrane size or surface area, a simple model incorporating major gas phase reactions in the gasifier and hydrogen permeation via mixed proton-electron conducting materials was developed.

A mass balance for the feed side of the membrane tube yields

$$\frac{\partial F_i}{\partial x} - R_i + J_i = 0 \quad (1)$$

where F_i is the molar flow rate of component i , x is the length of the membrane tube, R_i is the reaction rate for forming component i , and J_i is the permeation rate of component i .

To evaluate R_i , chemical kinetics was employed to describe the rates of gas reactions in the feed side of the membrane. This approach was used by Karim and Metwally [11] satisfactorily for modeling of the reforming of natural gas. A reaction scheme comprising 14 chemical species and 32 elemental reaction steps has been employed. The chemical species considered are six major gas components in the gasifier: CH_4 , O_2 , CO , H_2 , CO_2 , and H_2O , and eight radicals: OH , CH_3 , H , O , HO_2 , H_2O_2 , CH_2O , and CHO . Because reforming reactions without catalysts are not expected to occur even at the gasification temperature of 1000°C , catalytic reaction kinetics was used in the model calculations.

In a simplified form, the hydrogen flux can be expressed in the form of the Wagner equation [12,13]:

$$J_{H_2} = -\frac{RT}{4F^2L} \frac{(\sigma_{H^+})(\sigma_{el})}{\sigma_{H^+} + \sigma_{el}} (\ln(p_{H_2}^f) - \ln(p_{H_2}^p)) \quad (2)$$

where R is the gas constant, F is the Faraday constant, L is the membrane thickness, σ_{H^+} is the proton conductivity, σ_{el} is the electronic conductivity, $p_{H_2}^f$ is the partial pressure of hydrogen in the feed side of the membrane and $p_{H_2}^p$ is the partial pressure of hydrogen in the permeate side. The membrane ambipolar conductivity was determined from the hydrogen permeation data measured in this project. The ambipolar conductivity values calculated from Eq. (2) based on the hydrogen flux of the SCTm membrane are shown in Figure 18. Although the conductivities vary with the pressure, a constant value of 0.05 S/cm was used for the calculation. The membrane thickness was assumed to be 25 micron , which is considered achievable with the current fabrication technologies.

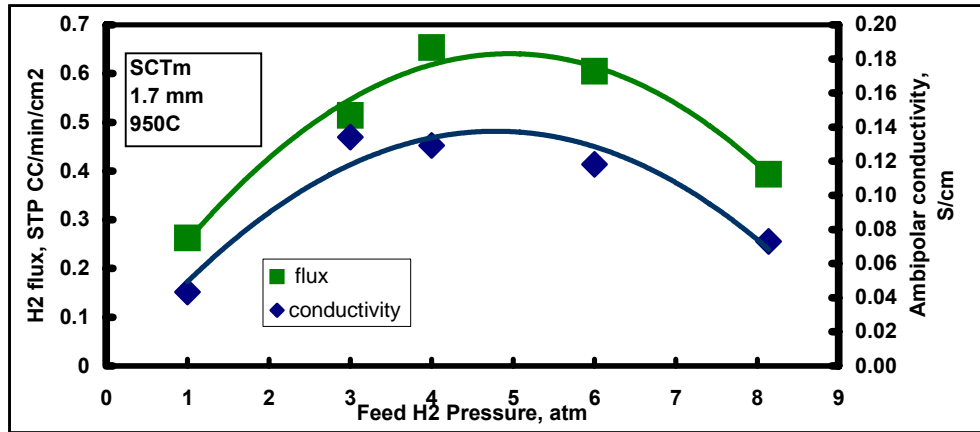


Figure 18. Hydrogen flux and calculated ambipolar conductivity for the SCTm membrane

Equation (1) can be solved with the typical numerical techniques. The required boundary conditions are the flow rates and the compositions of the coal syngas entering the membrane tubes. A GTI gasification model U-GAS[®] was used to estimate the gas flow rates and the compositions from a fluidized bed gasifier, which are listed in Table 1 along with other operating conditions and parameters. The Illinois #6 coal was used for this example.

Table 1. Summary of design parameters for the conceptual membrane gasification reactor

| | | | |
|----------------------------------|-------|------------------------------------|--------|
| coal feed, TPD | 1000 | temperature, C | 1100 |
| oxygen feed, TPD | 600 | pressure, atm | 60 |
| steam feed to gasifer, TPD | 595 | gasifier diameter, cm | 330 |
| steam feed to shift reactor, TPD | 270 | membrane tube diameter, cm | 1.25 |
| coal syngas flow rates, Nm/hr | 97125 | membrane thickness, cm | 0.0025 |
| coal syngas composition | | membrane tube length, cm | 900 |
| H ₂ | 0.280 | number of membrane tubes | 21300 |
| CH ₄ | 0.042 | membrae area, m ² | 7550 |
| CO | 0.297 | ambipolar conductivity, S/cm | 0.05 |
| CO ₂ | 0.146 | gas residence time of mem., sec | 8 |
| H ₂ O | 0.236 | enclosing filter tube diameter, cm | 1.87 |

The gasifier diameter without the membrane module calculated from GTI's gasification model was about 2.5 meter. To accommodate the membrane unit, the upper section of the gasifier was increased to 3.3 meter in diameter. It appears that a membrane module can be configured within a fluidized bed gasifier without a substantial increase of the gasifier dimensions. If multi-train of gasifiers are used for the 1000 TPD coal to hydrogen plant, the gasifier diameter and the associated number of membrane tubes will be reduced.

In this design example, the membrane gasification reactor produces 44240 Nm³/hr of hydrogen and 46610 Nm³/hr of non-permeable syngas with the following compositions: 4% H₂, 0.8% CH₄, 39% CO, 40% CO₂, and 16% H₂O. A significant amount of CO still exists in the non-permeable stream. Further optimization and process options for recovering more hydrogen from the non-permeable syngas stream will need to be developed. The performance of this membrane configuration will be used in the simulation for the overall coal to hydrogen processes employing the membrane reactor in Task 3.

Task 3 – Process Evaluation and Flow Sheet Development

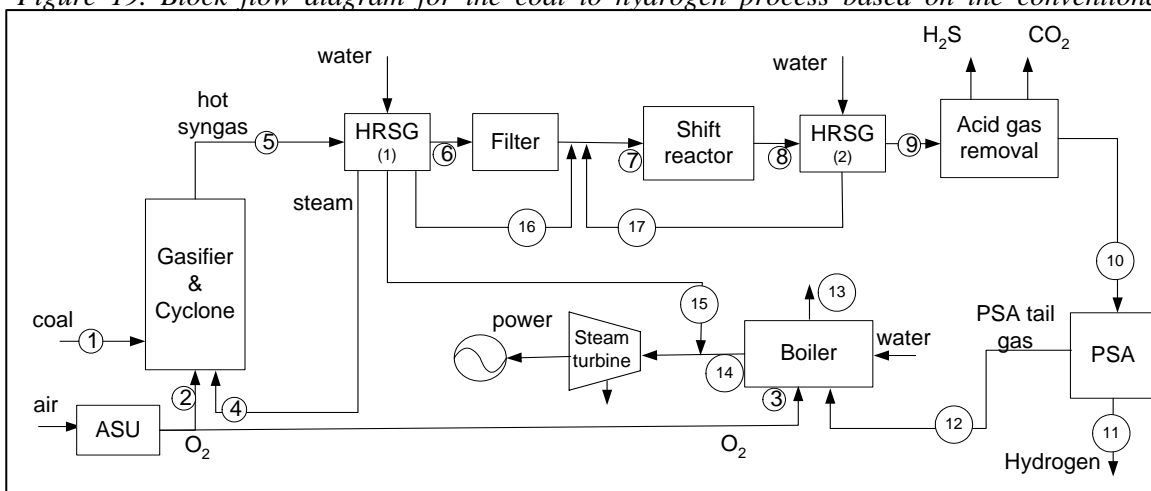
Flowsheet simulation was performed to calculate material and energy balances based on four hydrogen production processes from coal using high temperature membrane reactor (1000°C), low temperature membrane reactor (250°C), or conventional technologies. The commercial HYSYS simulator was used for the task. The design was based on a coal feed of 1000 TPD (Tons per Day) using Illinois #6 coal. GTI's U-GAS[®] fluidized bed was used for the gasifier, operating at 60 bars and 1100°C. Oxygen, instead of air, was used

for the gasifier oxidant. Air separation was based on the conventional cryogenic process. In addition to the gasifier, oxygen was also used for the combustion of the waste gas for steam or power generation. The simulation also focused on the heat recovery to generate additional power from the steam cycle. For the membrane processes, gas turbines were used to recover the heating value of the high pressure nonpermeate stream. For comparison purpose, the hydrogen product was generated at 50 bars, with the required hydrogen compression for the membrane processes. Hydrogen compression from the membrane unit can be eliminated if high pressure steam is used as a sweeping gas. However, this option is not considered in this work. Brief description of the four hydrogen from coal gasification processes examined in this task is given below:

Process A

For the coal to hydrogen process using the conventional technologies, a block flow diagram is shown in Figure 19. The hot syngas from the gasifier passes through a HRSG (Heat Recovery Steam Generation) unit to cool to below 300°C. After the fine particulates are removed by a filter, the syngas stream is added with steam before entering the water-gas-shift reactor. Because the shift reactor is located upstream of the acid gas removal unit, a sulfur tolerant catalyst has to be used for the shift reactor unit. The shift reaction is assumed to reach equilibrium at the reactor adiabatic temperature, which results in a CO conversion greater than 80%. Although the acid gas removal unit is not defined in this simulation, conventional process such as Selexol can be used in this low temperature range. All of the H₂S and 80% of CO₂ are removed in the acid gas removal unit. The hydrogen recovery for the PSA unit is assumed to be 80%. The PSA tail gas, which still contains CH₄, H₂ and CO, is sent to a boiler for steam generation, which is then used for power generation in this case.

Figure 19. Block flow diagram for the coal to hydrogen process based on the conventional



technologies, Process A

Process B

The block flow diagram for the Process B, which utilizes a low temperature (<math><350^{\circ}\text{C}</math>) membrane shift reactor to replace the shift reactor and the PSA unit, is shown in Figure 20.

The low temperature membrane shift reactor in process B is modeled as a shift reactor and a hydrogen separation unit with part of its non-permeate or retentate stream recycled to the shift reactor. The hydrogen recovery for the separation unit is assumed to be 80% and 70% of the retentate is recycled back to the shift reactor. The hydrogen partial pressure in the permeate side is maintained at about 2 bar. The final hydrogen product is compressed to 50 bars, which is at about the same pressure from the PSA unit of the Process A.

Because sulfur tolerance of the membrane material (such as palladium) has not been proven, a warm gas clean up unit is placed upstream the membrane shift reactor. This gas clean up unit is mainly for the H_2S removal.

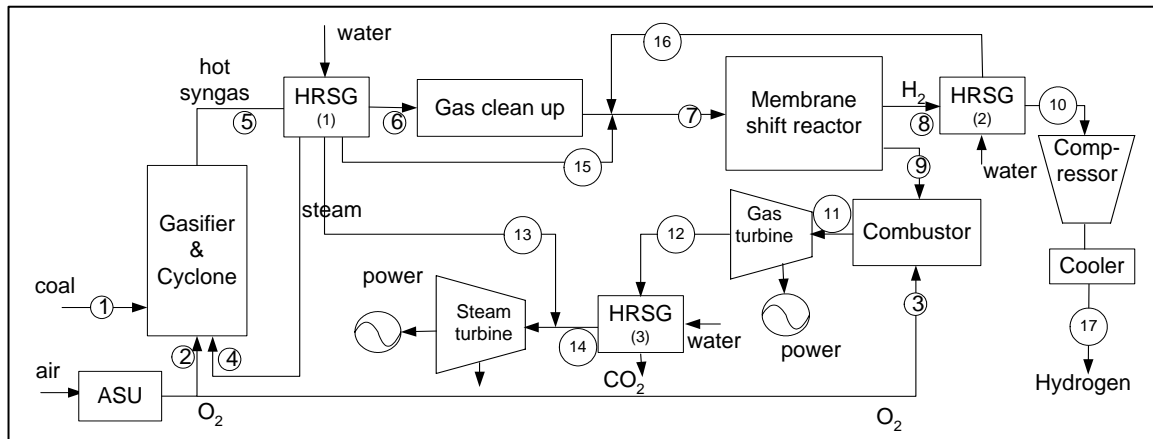


Figure 20. Block flow diagram for the coal to hydrogen process using a low temperature membrane shift reactor, Process B

The non-permeable gas from the membrane, which is at high pressure, ~ 50 bar, is sent to a gas turbine for power generation. Oxygen combustion at the high pressure is used to facilitate the CO_2 capture process. High pressure steam produced in the system is sent to a steam turbine for additional power generation.

Process C

Process C employs a high temperature H_2 -selective membrane such as the mixed protonic-electronic conducting membranes evaluated in this project. A block flow diagram of the Process C is shown in Figure 21.

The performance of the high temperature membrane reactor is based on the conceptual design and modeling of the tubular membranes, as reported in the Task 2 section. Although the membrane module can be configured within the freeboard region of the fluidized bed gasifier, it can also be closely coupled with the gasifier, as shown in Figure

21. Because no low temperature shift reactor is used in this process option, additional steam is added to the membrane module to facilitate reforming and shift reactions in the membrane reactor. Similar to the low temperature membrane shift reactor case in Process B, the hydrogen is produced at about 2 bars. Both hydrogen product and the non-permeable gas streams go through a HRSG and are cooled to about 270°C. After further cooling, the hydrogen product is compressed to about 50 bars.

The cooled non-permeable gas, after cleaned up for the removal of sulfur and other particulates, is sent to a combustor for power generation in a combined cycle, similar to the Process B.

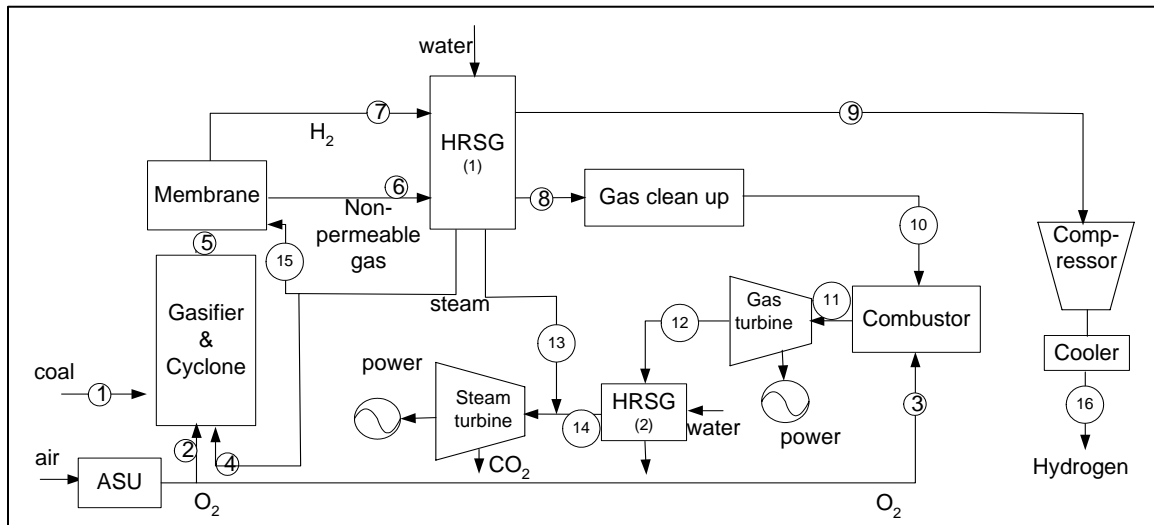


Figure 21. Block flow diagram for the coal to hydrogen process using a high temperature membrane reactor, Process C

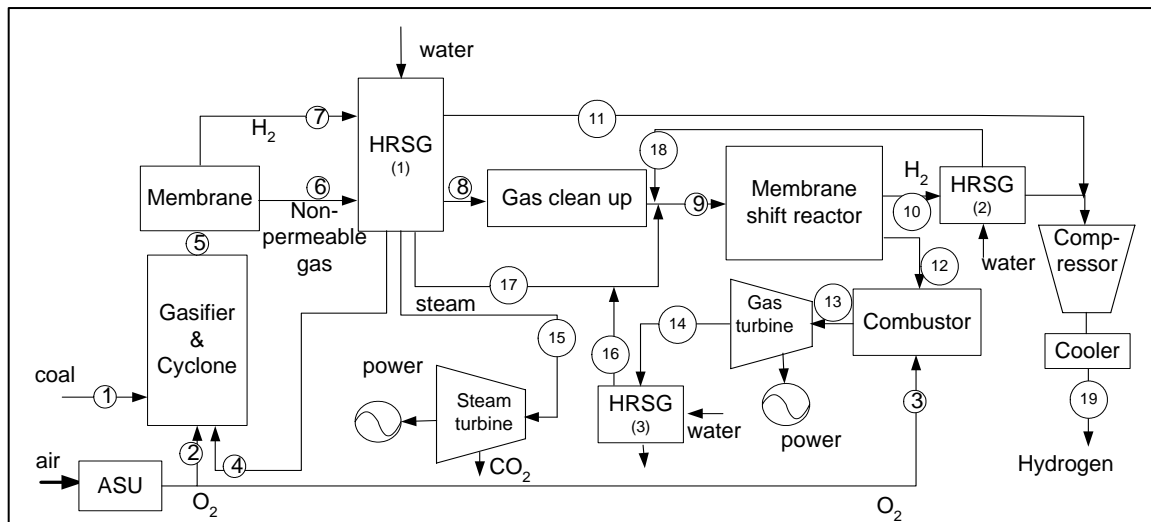


Figure 22. Block flow diagram for the coal to hydrogen process using a high temperature and a low temperature membrane reactors, Process D

Process D

Process D, shown in Figure 22 combines the high temperature membrane reactor in Process C and the low temperature membrane reactor in Process B to maximize the hydrogen production from coal gasification.

Again, the performance of the high temperature membrane reactor is based on the conceptual design reported in Task 2. The non-permeable gas from the high temperature membrane gasification reactor, after cooling and clean up is sent to a low temperature membrane reactor to further convert CO and separate H₂. The non-permeable gas from the low temperature membrane reactor is sent to a combustor for power generation in a combined cycle.

For comparative purpose, the performances of the different coal to hydrogen processes are evaluated by the cold gas efficiency and the effective thermal efficiency, both of which are defined below:

$$\text{Cold gas efficiency} = \frac{\text{hydrogen product heating value (HHV)}}{\text{coal heating value (HHV)}}$$

$$\text{Effective thermal efficiency} = \frac{\text{hydrogen product heating value} + \text{net power produced}}{\text{coal heating value}}$$

Table 2 summarized the amounts of hydrogen produced, power generated from the turbines, power consumption from the major equipment, the effective thermal efficiencies, the cold gas efficiencies and other parameters for the four processes evaluated in this work. In all four processes, CO₂ can be readily captured due to the use of oxygen. However, compression of CO₂ is excluded in the power calculation. Hydrogen product pressure is at 50 bars.

As can be seen, a less amount of oxygen would be required in the combustor to burn the waste gas when more hydrogen is produced in the process. Less power is produced when more hydrogen is generated. For the process employing both the high temperature and the low temperature membrane reactors (Process D), the hydrogen production can be increased by more than 50% relative to the conventional coal to hydrogen process (Process A), with a negative power output of 1 MW for a 1000 TPD plant. The conventional process has a net power output of 7 MW. For the process employing only the high temperature membrane reactor process (Process C), the hydrogen production is increased by about 10% relative to the conventional process, with a net power output of 15 MW. For the process employing only the low temperature membrane reactor process (Process B), the hydrogen production is increased by about 20%, with a net power output of 10 MW.

Process C or D also shows one advantage of the reduced syngas flows from the gasifier or from the high temperature membrane reactor to the syngas cooler, in comparison with Process A or Process B, which could potentially reduce the sizes of the downstream equipment such as gas clean up or shift reactor.

Table 2. Summary of performance for different coal to hydrogen processes

| Process | A conventional | B Low temp membrane | C High- temp membrane | D Low-temp & high- temp membrane |
|---------------------------------|-------------------|---------------------------|--------------------------------|--|
| coal feed, TPD | 1000 | 1000 | 1000 | 1000 |
| oxygen feed, kmole/hr | 1459 | 1279 | 1329 | 929 |
| gasifier | 779 | 778.9 | 779 | 779 |
| combustor | 680 | 500 | 550 | 150 |
| hydrogen product, kmole/hr | 1826 | 2177 | 2070 | 2896 |
| flow to syngas cooler, kmole/hr | 4270 | 4270 | 3156 | 2630 |
| steam turbine power, MW | 22 | 12 | 20 | 7 |
| gas turbine power, MW | | 21 | 19 | 14 |
| oxygen compressor, MW | 3 | 5 | 5 | 4 |
| ASU power, MW | 11 | 10 | 10 | 7 |
| hydrogen compressor, MW | | 8 | 7 | 10 |
| water pumps, MW | 0.5 | 0.4 | 0.4 | 0.2 |
| net power, MW | 7 | 10 | 15 | -1 |
| effective thermal efficiency, % | 46.3 | 55.6 | 54.4 | 69.8 |
| cold gas efficiency, % | 44.1 | 52.6 | 50 | 69.9 |

Task 4 – Economic Evaluation for Overall H₂ Production Process

Economic analysis was performed to evaluate the hydrogen product costs from the above four coal to hydrogen processes. Cost estimates for hydrogen production from coal based on the conventional technologies have been studied by several groups [1,2,14-16]. Itemized capital costs used for the current study in this project are based on those reported in the literature. These include the major equipment such as gasifier, heat recovery system, air separation (ASU) plant, gas clean up unit, shift reactor, PSA, turbines, etc. and are listed in Table 3. Obviously, the cost of each processing unit depends on the size. The size of the unit is determined by the quantities of the material, coal or syngas, that each unit can process, which is listed in the third column of the Table 3. For the high temperature membrane reactor unit in Process C or D, the membrane cost is assumed to meet the DOE's cost target of \$100/ft². Design study in Task 3 shows the required membrane area to be 7550 m² (see Table 1), which results in a total membrane cost of \$8124K. The membrane module is assumed to account for 40% of the membrane separation unit cost with the remaining 60% for the auxiliary equipment including hydrogen compressor. The total cost for the high temperature membrane unit is estimated to be \$20,300K.

Table 3. Itemized capital cost and corresponding equipment size

| unit | Cost \$1000K | size |
|--------------------------------|--------------|----------------------|
| coal preparation and handling | 32,000 | 2500 tpd coal |
| gasifier (fluidized bed) | 32,000 | 2500 tpd coal |
| Heat recovery steam generation | 7,400 | 259,000 Nm/hr syngas |
| shift reactor | 19,000 | 259,000 Nm/hr syngas |
| PSA | 34,000 | 259,000 Nm/hr syngas |
| ASU +O2 compressor | 50,000 | 2000 tpd O2 |
| gas cleanup + sulfur recovery | 30,000 | 259,000 Nm/hr syngas |
| gas turbine + combustor | 20,000 | 52 MW |
| steam turbine | 17,000 | 78 MW |
| balance of plant | 70,000 | 2500 tpd coal |
| low temp membrane + shift | 53,000 | 259,000 Nm/hr syngas |
| high temp membrane | 20,300 | 97,125 Nm/hr syngas |

Based on the flow rates of the material streams for the four processes shown in Figure 19, 20, 21 and 22, the cost of each piece of equipment can be calculated using the 0.6 scale factor. The numbers in Table 3 are used as the basis of the cost and the size of the equipment. For example, the gasifier cost for a 1000 TPD plant is \$32 million multiplied by $(1000/2500)^{0.6}$ or \$18.5 million. Instead of material flows, the power outputs are used to scale the costs of the turbines. The results for the capital cost of major equipment for the four processes are listed in Table 4.

The final hydrogen product cost is calculated using the IGCC Financial Model Version 4 developed by Nexant, Inc., which is available through DOE. The financial parameters used in the model are 30 years plant life, 95% plant availability, 3 years construction period, 80% debt and 20% equity, 39% tax rate, and 18% Internal Rate of Return (IRR). Other relevant cost parameters are cost of coal \$28/ton, cost of electricity \$30/MWh, and cost of annual operation 4% of capital cost. The calculated hydrogen costs are listed at the bottom of Table 4.

Process D, despite its higher capital cost, shows about 30% reduction in the hydrogen cost compared to Process A, because Process D produces more hydrogen for the given amount of coal feed. Process D has a lower ASU cost due to a smaller amount of waste gas to combust with O₂. The cost of gas clean-up unit is also lower. However, the capital cost is increased by the additional membrane units. Process B, similar to Parson's study, shows a cost advantage over the conventional coal to hydrogen process. Process C, with an advantage of lower capital than Process B, also has an about 15% cost saving from the conventional Process A.

Table 4. Summary of equipment size and capital cost for the four hydrogen production processes from coal gasification

| unit | Quantity of Material Processed | | | | Capital Cost, \$1000 | | | |
|------|--------------------------------|---|---|---|----------------------|---|---|---|
| | process | A | B | C | D | A | B | C |

| | | | | | | | | | |
|--------------------------------|--------------|--------|--------|--------|--------|---------|---------|---------|---------|
| coal preparation and handling | tpd coal | 1000 | 1000 | 1000 | 1000 | 18,470 | 18,470 | 18,470 | 18,470 |
| gasifier (fluidized bed) | tpd coal | 1000 | 1000 | 1000 | 1000 | 18,470 | 18,470 | 18,470 | 18,470 |
| Heat recovery steam generation | Nm/hr syngas | 95648 | 95648 | 117062 | 103152 | 4,070 | 4,070 | 4,600 | 4,260 |
| shift reactor | Nm/hr syngas | 116637 | 0 | 0 | 0 | 11,770 | 0 | 0 | 0 |
| PSA | Nm/hr syngas | 63773 | 0 | 0 | 0 | 14,670 | 0 | 0 | 0 |
| ASU +O2 compressor | tpd O2 | 1120 | 982 | 1020 | 710 | 35,320 | 32,630 | 33,390 | 26,860 |
| gas cleanup + sulfur recovery | Nm/hr syngas | 95648 | 95648 | 70694 | 58912 | 16,500 | 16,500 | 13,770 | 12,340 |
| gas turbine + combustor | MW | | 21 | 19 | 14 | 0 | 11,610 | 10,930 | 9,100 |
| steam turbine | MW | 22 | 12 | 20 | 7 | 7,940 | 5,520 | 7,500 | 4,000 |
| balance of plant | tpd coal | 1000 | 1000 | 1000 | 1000 | 40,400 | 40,400 | 40,400 | 40,400 |
| low temp mem + shift | Nm/hr syngas | | 112560 | | 74547 | 0 | 32,150 | | 25,100 |
| high temp mem | Nm/hr syngas | | | 95648 | 95648 | 0 | 0 | 20,290 | 20,290 |
| Total capital | | | | | | 167,600 | 179,800 | 167,800 | 179,300 |
| \$/kg H2 | | | | | | 1.38 | 1.19 | 1.15 | 0.96 |
| \$/MBtu H2 | | | | | | 9.70 | 8.40 | 8.12 | 6.75 |

CONCLUSIONS AND RECOMMENDATIONS

The major achievements from this project can be summarized as follows:

- Constructed and commissioned a new membrane permeation unit capable of operating at up to 1100°C and 60 bar, allowing screening and testing of hydrogen membranes under gasification conditions.
- The hydrogen flux measured for several proton-conducting perovskite membranes appeared to be adequate for the membrane module design. The highest hydrogen flux obtained was 1.0 STP cc/min/cm² for the SCTm membrane at 3 bars and 1040°C.
- Conceptual design of a membrane reactor for a plant of 1000 TPD coal showed that a membrane module could be configured within a fluidized bed gasifier without a substantial increase of the gasifier dimensions.
- Developed membrane reactor models for fluidized bed gasifier incorporating major gas phase reactions in the membrane gasifier and hydrogen permeation via mixed proton-electron conducting materials.
- Completed flowsheet simulation for hydrogen production based on the proposed membrane reactor processes and confirmed a more than 50% increase in hydrogen production efficiency compared to the conventional process.

- Identified the Zr-doped perovskite membrane as a leading material for further testing with respect to the chemical stability issues in the coal-derived syngas environment.
- The proposed membrane reactor process could potentially decrease the hydrogen cost by about 30% from the conventional coal to hydrogen process, based on a preliminary economic analysis.

GTI has developed a multi-year road map for moving this concept to commercial success. The plan calls for development efforts in four major areas, membrane material development, membrane module development, membrane gasifier process development, and membrane gasifier scale-up. In the initial phase of the program, the membrane material development is the key effort, which is the focus of this project. The membrane material developed in the laboratory must be fabricated in a commercial scale, which also depends on a careful design of the membrane module, either tubular or planar form. Membrane process development and optimization is essential to realize the maximum performance from the selected membrane materials and achieve the overall cost effectiveness. The developed membrane gasifier technology will be validated through a series of bench, pilot and commercial demonstration units. Recommendations for future works include:

- Improve the hydrogen permeability by minimizing the membrane thickness and increasing the material conductivity.
- Improve the chemical and mechanical stability of the membrane materials.
- Conduct permeation testing with simulated syngas
- Conduct permeation testing with real syngas from a coal gasifier
- Scale up the size of the membrane disks. Samples as large as 1.25" diameter disks have been routinely prepared in this program. Much bigger sizes will be needed for future commercial applications.

REFERENCES

1. Parsons Infrastructure and Technology Group, Inc., March 2002 "Hydrogen Production Facilities Plant Performance and Cost Comparisons", Final Report DOE Contract DE-AM26-99FT40465.
2. Gary, D and G. Tomlinson, Mitretek, July 2002 "Hydrogen from Coal", MTR 2002-31DOE Contract DE-AM26-99FT40465.
3. H. Iwahara, T. Esaka, H. Uchida, and N. Maeda, 1981. "Proton Conduction in Sintered Oxides and Its Application to Steam Electrolysis for Hydrogen Production" Solid State Ionics, 3/4, 359-363.
4. S. Doong, 2004 "Direct Hydrogen Production from Coal Using Novel Membrane Gasifier" ICCI project report 03-1/2.1A-2.
5. S.J. Doong, F. Lau and E. Ong, 2005 "Mixed Protonic-Electronic Conducting Membrane for Hydrogen Production from Solid Fuels" in "Advances in Membranes for Energy and Fuel Applications" ed. By A. Bose, ACS Book Series, in press.
6. J.F. Liu and A.S. Nowick, 1992 "The incorporation and migration of protons in Nd-doped BaCeO₃", Solid State Ionics, 50, pp131.

7. X. Qi and Y.S. Lin, 2000, "Electrical Conduction and Hydrogen Permeation Through Mixed Proton-Electron Conducting Strontium Cerate Membranes" Solid State Ionics, 130, P149.
8. S. M. Haile, G. Staneff and K. H. Ryu, 2001 "Non-stoichiometry, Grain Boundary Transport and Chemical Stability of Proton Conducting Perovskites", J. of Materials Science, 36, p1149-1160.
9. K. H. Ryu and S.M. Haile, 1999, "Chemical Stability and Proton Conductivity of Doped BaCeO₃-BaZrO₃ Solid Solutions" Solid State Ionics, 125, P355-367.
10. K. Katahira, Y. Kohchi, T. Shimura and H. Iwahara, 2000, "Protonic Conduction in Zr-Substituted BaCeO₃" Solid State Ionics, 138, P91-98.
11. G.A. Karim and M.M. Metwally, 1979. "A Kinetic Investigation of the Reforming of Natural Gas for the Production of Hydrogen", Int. J. Hydrogen Energy, Vol. 5, P293.
12. H.J.M. Bouwmeester and A.J. Burggraaf, 1996. "Dense Ceramic Membranes for Oxygen Separation", in Fundamentals of Inorganic Membrane Science and Technology, Ed. By A.J. Burggraaf and L. Cot, pp 435-528, Elsevier Science B.V.
13. T. Norby and Y. Larring, 2000. "Mixed Hydrogen Ion-Electronic Conductors for Hydrogen Permeable Membranes", Solid State Ionics, 136-137, pp139-148.
14. Nexant in association with GTI, March 2005, "Task 3 Gasification Alternatives for Industrial Applications" Final Report, DOE Contract No DE-AC26-99FT40342, Subtask 3.4 – Lignite Fueled IGCC Power Plant.
15. D. R. Simbeck and E. Chang, SFA Pacific, Inc., 2002, "Hydrogen Supply: Cost Estimates for Hydrogen Pathways – Scoping Analysis", NREL Report, DOE Contract No. DE-AC36-99-GO10337.
16. M. Schwartz, ITN Energy Systems, Inc., 2004, "Novel Composite Membrane for Hydrogen Separation in Gasification Processes in Vision 21 Energy Plants", Final Report, DE-FC26-01NT40973,

DISCLAIMER STATEMENT

This report was prepared by Francis Lau, Gas Technology Institute, with support, in part by grants made possible by the Illinois Department of Commerce and Economic Opportunity through the Office of Coal Development and the Illinois Clean Coal Institute. Neither Francis Lau, Gas Technology Institute, nor any of its subcontractors nor the Illinois Department of Commerce and Economic Opportunity, Office of Coal Development, the Illinois Clean Coal Institute, nor any person acting on behalf of either:

- (A) Makes any warranty of representation, express or implied, with respect to the accuracy, completeness, or usefulness of the information contained in this report, or that the use of any information, apparatus, method, or process disclosed in this report may not infringe privately-owned rights; or
- (B) Assumes any liabilities with respect to the use of, or for damages resulting from the use of, any information, apparatus, method or process disclosed in this report.

Reference herein to any specific commercial product, process, or service by trade name, trademark, manufacturer, or otherwise, does not necessarily constitute or imply its endorsement, recommendation, or favoring; nor do the views and opinions of authors expressed herein necessarily state or reflect those of the Illinois Department of Commerce and Economic Opportunity, Office of Coal Development, or the Illinois Clean Coal Institute.

Notice to Journalists and Publishers: If you borrow information from any part of this report, you must include a statement about the state of Illinois' support of the project.